

Did the Submarine, Across-Arc Normal Fault System in the Southwest Ryukyu Arc Trigger the 1771 Tsunami? Field Evidence from Multibeam Survey and In-Situ Observation

T. Matsumoto^{1*}, R. Shinjo¹, M. Nakamura¹, A. Doi¹, M. Kimura¹, T. Ono¹, A. Kubo²

¹Faculty of Science, University of the Ryukyus, Japan

²Faculty of Science, Kochi University, Japan

Received: 2 October, 2008

Accepted: 22 November, 2008

Abstract

Recent numerical simulation of tsunami propagation proposed a new hypothesis about the origin of the 1771 tsunami that devastated the southwest Ryukyu district of Japan; a slip of the East Ishigaki Fault, a 44km-long fault lying 50km off the east coast of Ishigaki Island, might be the cause of the 1771 tsunami. The present study is to test this hypothesis through visual observation by means of the precise seafloor image collected by the Hyper-Dolphin remotely operated vehicle. The hypothesis may be proved if definite evidence of a slip along the whole fault is obtained. Investigating the fault was accomplished by a reconnaissance survey at three representing fault segments: southern, central and northern. The result of the survey at the southern segment shows that the main fault scarp is covered by many large boulders. On the escarpment, 6m sections with a gradient of almost 90 degrees were observed. The result of the survey at the central segment shows similar characteristics as that at the southern segment. The northern segment was characterized by wide exposure of limestone outcrop with many cracks and fissures on the outcrop which represents nascent faulting. These facts suggest the northward propagation of the faulting along the main scarp. The result demonstrates that the amount of displacement at the fault segments is not uniform. This does not support the assumption taken into the numerical simulation; thus, it is unlikely that the slip at the fault generated the 1771 tsunami, even though simultaneous rupture at multiple fault segments are taken into account.

Keywords: submarine active fault, Yaeyama Earthquake Tsunami, East Ishigaki Fault, Ryukyu Islands

Introduction

The Ryukyu Arc is located on the southwestern extension of the Japanese Island-arc toward the east of Taiwan along the margin of the Asian continent off China. The island-arc forms an arcuate trench-arc-backarc system with the strike of N30-40°E in the northeastern-central area and

N70-90°E in the southwestern area (Fig. 1). A N54°W subduction of the Philippine Sea Plate at a rate of 6-8 cm/y relative to the Eurasian Plate [1] causes frequent earthquakes along the island-arc. The Philippine Sea Plate is subducting almost normally in the northeastern-central area and more obliquely around the southwestern area. Behind the arc-trench system, the Okinawa Trough was formed by back-arc rifting, where active hydrothermal vent systems have been discovered [e.g. 2, 3] and geochemical and biological studies on some of these sites are still now going on.

*e-mail: tak@sci.u-ryukyu.ac.jp

A M7.4 earthquake and the subsequent devastating tsunami called ‘Yaeyama Earthquake Tsunami’ or ‘Great Meiwa tsunami’ (‘Meiwa’ is one of the names of the historic era in the Japanese dating system) attacked the southwestern Ryukyu Island region (Yaeyama Islands and Miyako Islands) on 23 April 1771. The tsunami recorded some 12,000 casualties in these districts. It is of great importance to locate the source area of this tsunami for tsunami hazard mitigation in the future. However, the source area of the tsunami has not yet been specified completely, although much effort of numerical simulation of tsunami propagation [4, 5], on-land study to get information of the distribution of tsunami boulders that are transferred from undersea area onto land by tsunami [6], submarine survey expeditions [7-9], etc. has been conducted in order to get the solution to fit the distribution of the tsunami inundation height recorded in the historical local documents. The details of the problems in these past studies are reported in [10].

Hydrographic survey including bathymetric mapping and seismic reflection surveys by the Hydrographic Department, Maritime Safety Agency of Japan (present ‘Japan Coast Guard’) in the 1970’s [11] revealed many submarine active faults in the southwestern Ryukyu area. Most of them are normal faults completely crossing the Ryukyu arc. One of these normal faults crossing the Ryukyu Arc is located about 50km off the eastern coast of Ishigaki Island. We tentatively call this ‘East Ishigaki Fault.’ This is a NW-SE trending submarine normal fault with ~40km length, which may cause an M7-class earthquake. The identified submarine active faults together with the on-land active faults were compiled and listed in [12] with their detailed descriptions. The East Ishigaki Fault is one of the ‘officially’ identified submarine active faults in [12]. Nakamura [13] proposed through the numerical simulation of tsunami propagation that an 8-m slip along this fault can cause the ‘1771 Yaeyama Earthquake Tsunami’ and reasonably explains the inundation level and distribution revealed from field evidence in the southwestern Ryukyu Islands [6].

Since the East Ishigaki Fault can be the origin of the 1771 tsunami, a precise topographic survey by SEABAT8160 multibeam echo sounder and an underwater geological survey by use of the remotely operated vehicle (ROV) Hyper-Dolphin were carried out from 3-8 May 2005 during NT05-04 Leg2 Expedition by R/V NATSUSHIMA operated by JAMSTEC (Japan Agency for Marine-Earth Science and Technology)/NME (Nippon Marine Enterprises, Inc.) [10]. Based on the result of the precise swath bathymetry, three sites around fault scarp, representing the southern, central and northern part of the fault, respectively, were selected for seafloor observation and sampling by the ROV. Fig. 2 shows the ROV tracks (Dive Nos. 405, 406, and 407) overlain on the seafloor topographic map [10].

In [10] the authors reported detailed description of the topographic features along the fault and an outline of the description of these three profiles of the ROV dives. After the previous report, more detailed description of the video image collected during these dives became available.

Table 1. Outline of the ROV Hyper-Dolphin dives during the NT05-04 cruise by R/V NATSUSHIMA. Both offshore facilities are operated by the Japan Agency for Marine-Earth Science and Technology (JAMSTEC).

Dive No. 405 (04 May 2005)	Latitude	Longitude	Time	Depth
Landing	24°24.990’N	124°37.509’E	09:02	442m
Left Bottom	24°25.150’N	124°38.628’E	16:09	385m
Dive No. 406 (05 May 2005)	Latitude	Longitude	Time	Depth
Landing	24°28.002’N	124°33.565’E	08:51	421m
Left Bottom	24°28.864’N	124°34.665’E	12:50	330m
Dive No. 407 (07 May 2005)	Latitude	Longitude	Time	Depth
Landing	24°35.607’N	124°26.961’E	13:27	316m
Left Bottom	24°35.068’N	124°25.474’E	18:01	325m

In this article the authors will report the updated video image description which is essential to identifying the activity and the evolution history of the fault and to discuss the possibility of generating a large-scale tsunami. High-definition television (HDTV) video image from the ROV dives, navigation data, rock samples collected during the dives were used in this study. The outline of ROV dives is shown in Table 1.

The precise topographic survey by SEABAT8160 multibeam echo sounding revealed the topographic relief of the whole fault and located its northwestern and southeastern termini [10] (Fig. 2). The northwestern terminus of the fault is at 24°38’N, 124°23’E, and the southeast end is

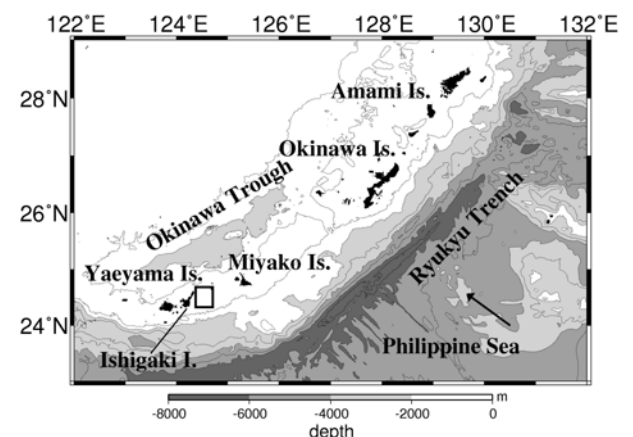


Fig. 1. Simplified topographic map of the Ryukyu Islands. Topographic data are from the 500m-gridded data compiled by the Japan Coast Guard. The box on the map shows the study area and corresponds to the area of Fig. 2. ‘I.’ stands for ‘Island’ and ‘Is.’ stands for ‘Islands’.

branched into two from 24°22'N, 124°40'E, and extends to two termini, up to 24°20'N, 124°40.3'E and 24°21'N, and 124°41'E, respectively. The total length of the fault is about 44km [10]. The research expedition also revealed that the fault consists of five segments bounded by kinking of the fault strike [10].

Data Analyses

Geological Cross Sections and Route Mapping

Primarily, the obtained HDTV video images along the three tracks were analyzed in order to detect the most recent deformations of the seafloor. Especially noticeable were the spots where sedimentation status of the seafloor materials changes drastically. Also, the property and location of the collected rock samples [10] were taken into account for analysis and interpretation of seafloor deformation.

In order to detect the precise topographic features and sedimentation structures and to identify the location of recent/fossil seafloor deformation around the East Ishigaki Fault, geological cross sections were created for the three dives at the same vertical/horizontal scales for comparison.

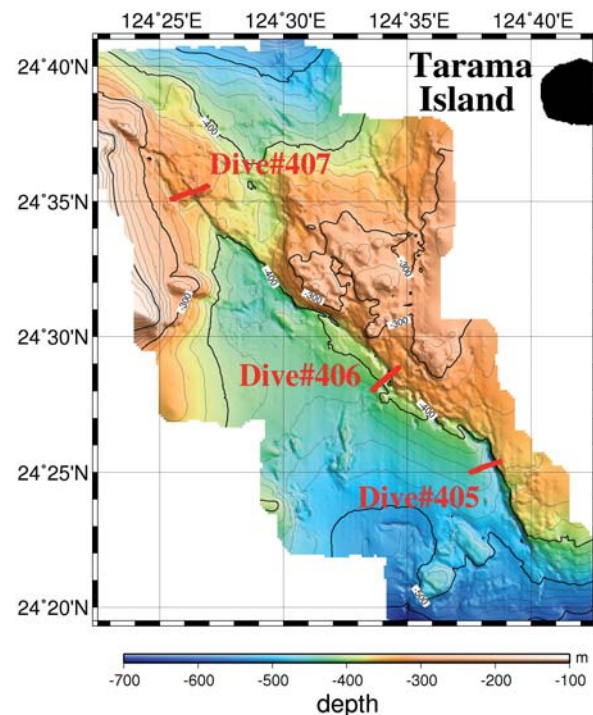


Fig. 2. Topographic map of the East Ishigaki Fault based on the sounding by SEABAT8160 system on board NATSUSHIMA during NT05-04 cruise [10] and NT08-14 cruise. The length of the fault is 44 km, which corresponds to an M-7 class earthquake. The fault consists of 5 segments bounded by kinks of each strike. Three dive tracks by ROV Hyper-Dolphin (Dive Nos. 405, 406 and 407) are overlain on the topographic map.

The data used to draw the vertical cross sections were based on water depth (every 10 seconds) and distance from the beginning point of the survey on the sea bottom at each point. Water depth was calculated by adding the raw depth data (in m) and the raw altitude data (in m) obtained from ROV meters. The distance was calculated by converging from the ROV position data (X: north, Y: east) with reference to the origin point of drawing the tracks into latitude and longitude. Then the acoustic positioning noise effect was filtered out. Finally, the distance from the beginning point of the seafloor survey was calculated.

Strikes of the Cracks

During Dive No. 407 a lot of cracks and fissures were observed; thus the position (the time), strike, and the number of these cracks were statistically analyzed. The strike of the crack on the monitor was determined by taking account of the HDTV camera azimuth which was superimposed onto the video image on the screen to get the strike of the crack. However, crack length was not considered for statistical analyses because it cannot be identified on the ROV video image. (Therefore, only the statistics of the strike are drawn on the rose diagrams.)

Description of the Dives

Dive No. 405 at the Southern Segment

Fig. 3 shows the vertical cross-section of the Dive No. 405 track. The seafloor along the whole track was covered with sediment. The starting point of the track was about 1,600m west of the main fault scarp. The seafloor around there was flat and ripple marks were observed around the location (Fig. 3 (b) - Photo A). The direction of the ripple marks was not uniform. The bottom material was fine-grained sand. As approaching the main fault scarp, the amount of granules-pebbles within the sand and the grain size also increased towards the main fault scarp (cf. Fig. 3 (b) - Photo B: fragment diameter increased from 1 cm to several cm). Much rubble was observed on the trough floor with coarse-grained sand and brecciated rock fragments (Fig. 3 (b) - Photo C). The depth of the trough bottom was about 38 m. An almost vertical slip surface where the basement rocks are exposed was observed in the central part of the escarpment (Fig. 3 (b) - Photo D). Above, the slope was steep but relatively smooth with fewer undulations (Fig. 3 (b) - Photo E). Most of the rocks collected from the rubble deposits which were deposited on the basement were calcareous conglomerate and limestones [10]. Water depth on the flat bottom with ripple marks was about 450m and was almost constant. Depth increased gradually as the ROV approached the main fault scarp. Maximum depth at the trough axis was 480m. After passing the main fault scarp, the gradient of the seafloor became small and a flat bottom appeared about 300 m away from the eastern edge of the scarp, where boulders (about 3m in diameter) were observed (Fig. 3 (b) - Photo F).

Dive No. 406 at the Central Segment

Fig. 4 shows the cross-section of Dive No. 406 track. A basement limestone is exposed at the starting point of the track. The seafloor became gradually shallower by about 50m along the first 1,500 m in distance then became deeper towards the trough facing the main fault (Fig. 4). This is different from the topographic profile along the Dive No. 405 track, where the depth was almost constant around the starting point and then increased near the main fault toward the trough (cf. Fig. 3). The basement was covered slightly with fine silt at the starting point (Fig. 4 (b) - Photo A). Ripple marks began to appear 400 m away from the starting point (Fig. 4 (b) - Photo B). The direction of the ripple mark was not constant. Angular boulders were deposited on the seafloor at the trough (Fig. 4 (b) - Photo C). Sediment was hardly observed and a basement was exposed on the fault scarp (Fig. 4 (b) - Photo D). Ripple marks and a coarse-grained sand deposit were observed around the vicinity of the edge of the main fault scarp (Fig. 4 (b) - Photo E). The relative height of the trough was about 29 m and water depth at the trough was 421m. Of the 11 rock samples collected during the dive, 6 were sandy limestones, 2 were clastic limestone, and the others were sandy porous limestone, sandy conglomerate, and limestone [10]. Fewer boulders than in Dive No. 405 were observed on the track.

Dive No. 407 at the Northern Segment

Water depth varied from 350m to 315m along the whole track; the undulation of the seafloor was rather poor compared with the other two dives (Fig. 5). The seafloor was characterized by extensive exposure of basement rock. Sediments were observed on the trough only, 750m and 2,500m away from the starting point. In the latter case, ripple marks with various direction were observed (Fig. 5 (b) - Photo B). These two locations with sediment were different from the location of the main fault. No fine-grained sands nor coarse-grained sands were deposited around the main fault. Seafloor undulation was rather remarkable around the main fault (Fig. 5 (b) - Photo E). Numerous cracks with the strike of roughly NNW and NW were observed on the basement. Some cracks were filled with sediment but others not (Fig. 5 (b) - Photo C/E). On the seafloor about 2,000 m away from the starting point, angular and rounded pebbles were deposited (Fig. 5 (b) - Photo D). Of the 8 collected rock samples, 4 were sandy porous limestone, 2 were clastic limestone, and the other two were calcareous algal limestone [10].

Statistics of the Cracks Observed During Dive No. 407

In order to test the difference in characteristics of the many cracks observed during Dive No. 407, average and

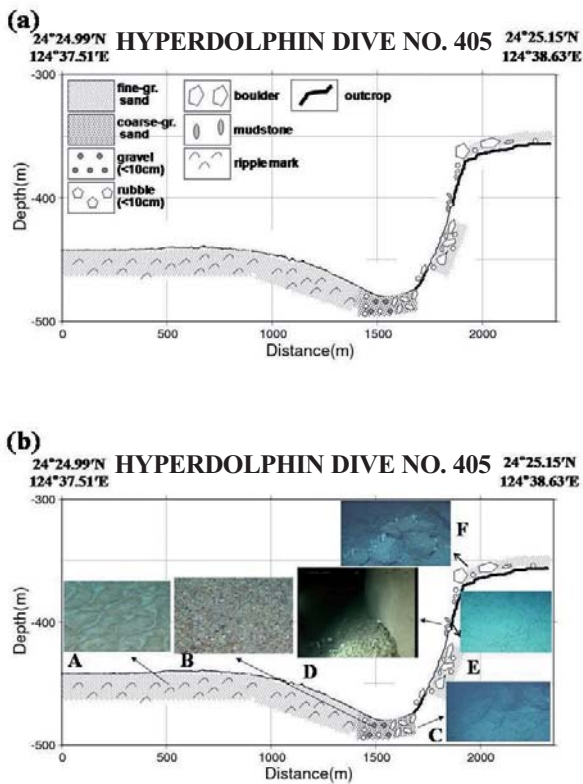


Fig. 3. (a) Topographic relief and geological cross section along the track of Dive No. 405 with the legend of the geological units. '-gr.' stands for '-grained'. (b) Same as (a) but with some representative seafloor image at each location.

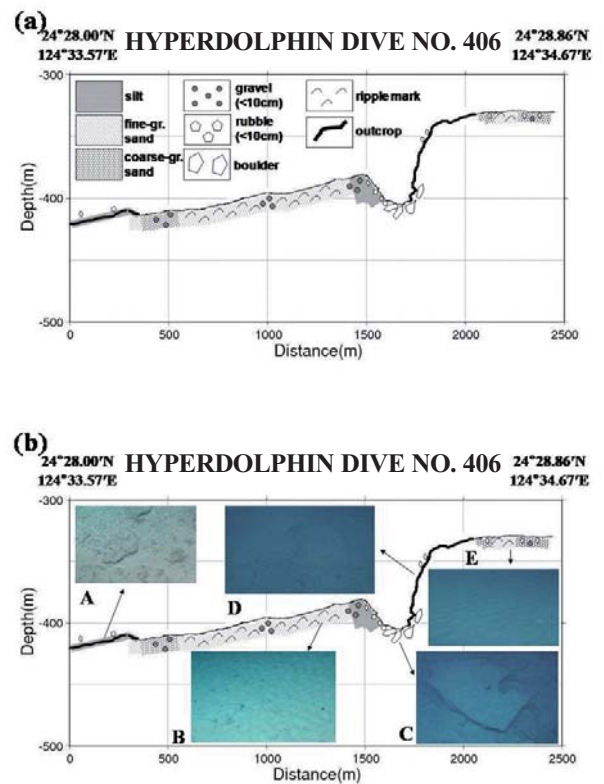


Fig. 4. (a) Topographic relief and geological cross section along the track of Dive No. 406 with the legend of the geological units. (b) Same as (a) but with some representative seafloor image at each location.

standard deviation of their strike were calculated. The cracks along the whole track of Dive No. 407 counted 255. The average and standard deviation of the strike of the cracks were 323.27° and 15.79° , respectively (Fig. 6 (a)). Next, the track was divided into two: east and west of the main fault. On the east side (Area 1), the cracks counted 142, and the average and standard deviation were 324.42° and 10.06° , respectively (Fig. 6 (b)). On the west side (Area 2), the cracks counted 113, and the average and standard deviation were 321.82° and 20.78° , respectively (Fig. 6 (b)).

Standard deviation is higher (more “dispersed”) in Area 2 than in Area 1. In order to verify the localization of the dispersion of the cracks, Area 2 was subdivided into two: Area 2-1 on the eastern half and Area 2-2 on the western half. In Area 2-1 the cracks counted 60, and average and standard deviation were 328.57° and 23.37° , respectively. In Area 2-2 the cracks counted 53, and average and standard deviation were 314.18° and 13.87° , respectively. The cracks were thus more dispersed near the main fault (Fig. 6 (c)). The length of the cracks could not be measured from the video image of the ROV because the viewport is limited to a few~several meters square. Therefore, the statistics do not include the information of the length of the cracks and the rose diagrams in Fig. 6 shows directions only.

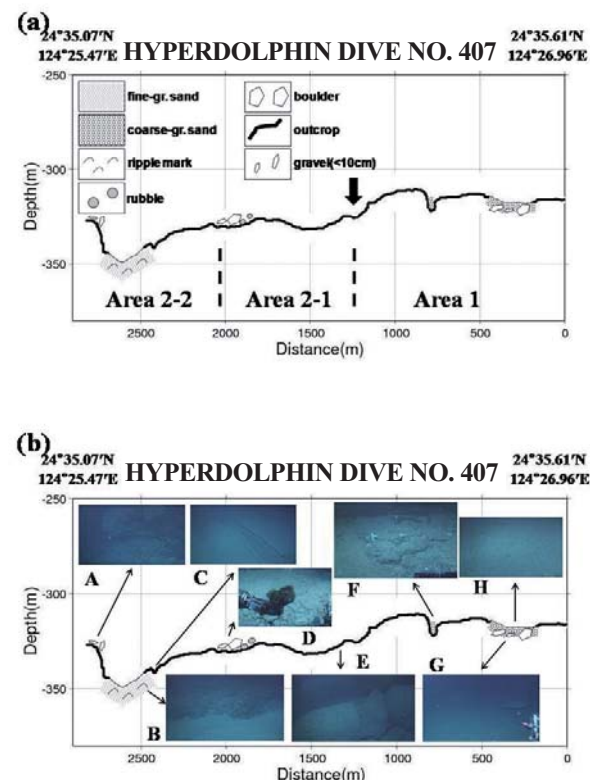


Fig. 5. (a) Topographic relief and geological cross section along the track of Dive No. 407 with the legend of the geological units. Thick arrow indicates location of the main fault extended from the southern segments. Area 1, 2-1 and 2-2 are the subdivided areas for statistics of the strike of the cracks (cf. Fig. 6). (b) Same as (a) but with some representative seafloor image at each location.

Discussion and Conclusion

Most of the rock samples collected from the basement outcrop were limestone blocks (or calcareous sedimentary rocks) except for a few from the trough, as reported in [10]. The starting point of Dive No. 405 on the footwall was covered with fine-grained sand with ripple marks. In Dive No. 406 a limestone basement was observed at the starting point away from the fault scarp instead of fine-grained sand. Fine-grained sand with ripple marks was observed toward the main scarp. In these two dives a limestone basement was observed on the main scarp and on the footwall. These suggest that basically both the footwall and the hanging wall are composed of the same material, that the whole study area is characterized by Ryukyu limestone exposure

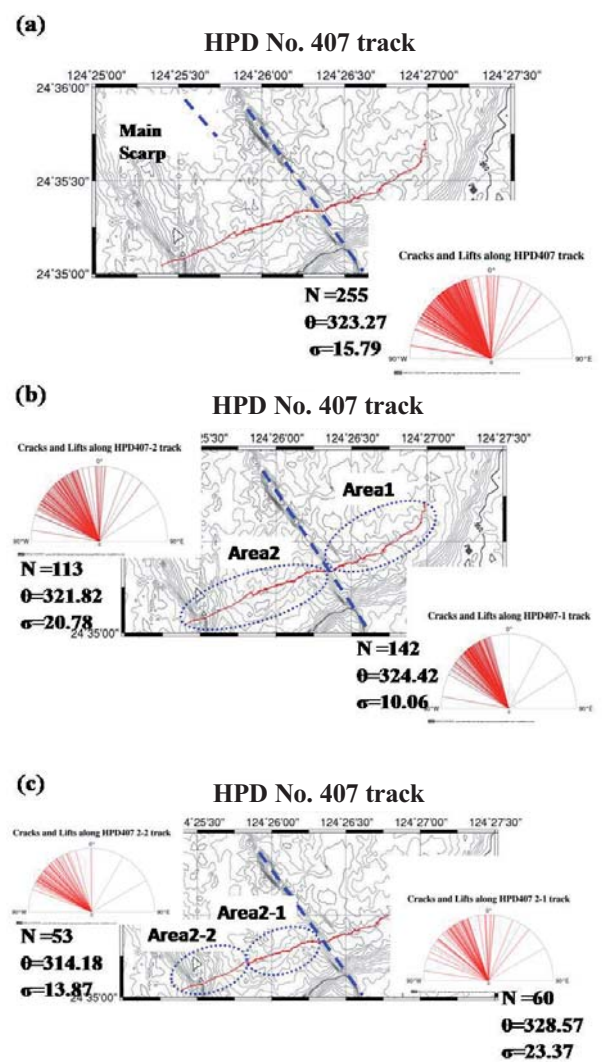


Fig. 6. Track of Dive No. 407 (red line on the map) and statistics of the strike of the fissures and cracks observed along the track. Blue line shows the location of the main fault scarp. (a) Along the whole track. (b) Comparison between the area east of the main fault (Area 1) and west of it (Area 2). (c) Comparison between the eastern half of Area 2 (Area 2-1) and the western half (Area 2-2). The number of the cracks (N), average and standard deviation of the strike of the cracks (θ and σ , respectively) are also shown on this figure.

and that the basement was split by the across-arc normal fault. Coarse-grained sand and gravel/rubble were observed towards and on the trough. On the main scarp an outcrop of limestone basement was exposed and in some part it was broken into rubble. These facts suggest that crash of the basement due to the fault slip is taking place repeatedly on the scarp and the trough. The fine-grained sand observed in Dive Nos. 405 and 406 might be the final product by the process of the crash of the limestone basement.

Relics of a 6m vertical slip were observed in the central part of the fault scarp in Dive No. 405. If earthquakes of similar magnitude occur repeatedly by a similar amount of slip, the total displacement of a couple of hundred meters along the fault may be the cause of more than several tens of repeated earthquakes. As observed during Dive No. 405, the cumulative displacement of the main fault of the East Ishigaki Fault is some 120m. Therefore, it can be concluded that the southern segment was formed by at least 20 major slips.

The relative height of the fault scarp is largest on the southern segment and second largest on the central segment. In the northern segment the topographic relief along the fault is very poor compared with the other two segments. Considering also that the basement is exposed along the whole track in Dive No. 407, the segment is in the earliest stage of the formation process of the fault. A reversed V-shaped topographic depression around 24°33'N, 124°28'E (Fig. 2) also suggests a propagation of faulting toward the north. Then it can be concluded that the East Ishigaki Fault formed first at the southernmost part and the faulting was propagated NNW to form the present 44-km-long fault. Propagation of the faulting north is also consistent with the stress model by [14]. If this is the case, and considering that the fault is segmented, propagation might take place episodically rather than continuously. This hypothesis may be tested by dating the collected limestone samples and by investigating the relationship between the date and location (depth).

The statistics of the strike of the cracks observed in Dive No. 407 show that Area 1 and Area 2-2 show similar standard deviation (10.1 degrees and 13.9 degrees, respectively). Standard deviation is much higher in Area 2-1 (23.4 degrees) compared with that of the other two areas. If these three areas are composed of limestone with the same physical properties and under the same regional stress field, the difference in the standard deviation of the strike of the cracks should be due to the different process which is taking place among these areas. Area 2-1 is the northern extension of the hanging wall of the main fault scarp where the evolution of the basement might be maximum across the fault, as suggested by the result of dive nos.405 and 406. Then the dispersion of the strike of the cracks in this area is considered to be the earliest stage of the crash of the basement and forming the hanging wall of the main fault scarp.

In order to test the hypothesis that the slip of the East Ishigaki Fault generated the 1771 Yaeyama Earthquake Tsunami [13], the reconnaissance survey along the fault by ROV Hyper-Dolphin was carried out. The inundation height

record of the tsunami based on the distribution of the tsunami boulders [6] is consistent with the result of the numerical simulation of the tsunami propagation [13], under the assumption that the length of the fault is some 40-50km (corresponding to an M7-class earthquake). However, the present study showed that the main fault is not a single fault but is segmented with different stages of faulting and deformation. Thus the result does not always support the assumption that all the segments formed at one time and that all the segments slipped at one time or with the same amount of displacement. The northern segment (Dive No. 407 site) appears to represent the nascent stage of faulting, judging from the observation of many open cracks on the exposed limestone basement. However, vertical displacement at this site is small compared with that at the central and southern segments. Therefore, it is difficult to consider that this segment generated a large-scale tsunami. Finally, it is concluded that the East Ishigaki Fault, which was the target of this work, was not the main source of the 1771 tsunami generation, but the possibility of some contribution to the tsunami remains. Another possible source of the tsunami is simultaneous rupture of the southern and central segments. However, considering the result of the numerical simulation [13], the amount of the slip should be larger (more than 10m) in order to fit the observed and calculated runup heights.

Some recent geohazards show that a landslide or a slump is associated with an identified active fault. The examples are the 17 Feb. 2006 Leyte Island (the Philippines) landslide, the 17 Jul. 1998 Papua New Guinea Earthquake and Tsunami, and the 17 July 2006 Java Earthquake and Tsunami. In the latter two cases, both faults and underwater landslides played a crucial role in generating a large-scale tsunami [15]. The topographic map of the present study area (Fig. 1) also shows relics of an underwater landslide at 24°32' N, 124°31'E. Therefore, an additional offshore survey and comparison of the result with that of similar cases might be essential to investigate the effect of the landslide associated with the fault slip as a potential source of a large-scale tsunami hazard.

Acknowledgment

The authors would like to thank the crew members of R/V NATSUSHIMA, the ROV operation team, and the onboard marine technician team for their technical support for this study. The authors also thank the members of the Ship Operation Department of the Japan Agency for Marine-earth Science and Technology (JAMSTEC) and Nippon Marine enterprises Inc. (NME) for their help in cruise planning. This study was financially supported by a Grant-in-Aid for Scientific Research (C), No. 18540425, and by Japan Society for the Promotion of Science (JSPS).

References

- 1 SENO T., STEIN S., GRIPP A.E. A model for the motion of the Philippine Sea Plate consistent with Nuvel I and geological data. *J. Geophys. Res.* **98**, 17941, 1993.

- 2 KIMURA M., OOMORI T., IZAWA E., KATO Y., ONO T., TANAKA T., KOIKE T., NISHIOKA S. Newly found vent system and ore deposits in the Izena Hole in the Okinawa Trough, Japan. *JAMSTEC J. Deep Sea Res.* **8**, 87, **1990**.
- 3 MATSUMOTO T., KINOSHITA M., NAKAMURA M., SIBUET J.C., LEE C.S., HSU S.K., OOMORI T., SHINJO R., HASHIMOTO Y., HOSOYA S., IMAMURA M., ITO M., TUKUDA K., YAGI H., TATEKAWA K., KAGAYA I., HOKAKUBO S., OKADA T., KIMURA M. Volcanic and hydrothermal activities and possible "segmentation" of the axial rifting in the westernmost part of the Okinawa Trough - preliminary results from the YOKOSUKA / SHINKAI 6500 Lequios Cruise -. *JAMSTEC J. Deep Sea Res.* **19**, 95, **2001**.
- 4 HIYOSHI Y., ANDO M., KIMURA M. Generation mechanism of the 1771 Nanseishoto Great Meiwa Tsunami – generation of a large-scale underwater landslide - Abstract Volume of the Annual Meeting of the Seismological Society of Japan pp. 80, **1986**.
- 5 HIRAISHI T., SHIBAKI H., HARA N. Numerical simulation of Meiwa-Yaeyama Earthquake Tsunami in landslide model with circular rupture. *Proc. Coastal Engin., Japan Society Civil Engineering* **48**, 351, **2001**.
- 6 KAWANA T., NAKATA T. Timing of late Holocene tsunamis originated around the southern Ryukyu islands, Japan, deduced from coralline tsunami deposits. *J. Geography* **103**, 352, **1994**.
- 7 MATSUMOTO T., KIMURA M. Detailed bathymetric survey in the sea region of the estimated source area of the 1771 Yaeyama Earthquake Tsunami and consideration of the mechanism of its occurrence. *J. Seismol. Soc., Japan, Second Series*, **45**, 417, **1993**.
- 8 MATSUMOTO T., UECHI C., KIMURA M. Surface deformation at the origin area of the 1771 Yaeyama Earthquake Tsunami observed by the precise survey off Yaeyama districts, Ryukyu area. *JAMSTEC J. Deep Sea Res.* **13**, 535, **1997**.
- 9 MATSUMOTO T., KIMURA M., NAKAMURA M., ONO T. Large-scale slope failure and active erosion occurring in the southwest Ryukyu fore-arc area. *Natural Hazards and Earth System Sciences* **1**, 203, **2001**.
- 10 MATSUMOTO T., SHINJO R., NAKAMURA M., KIMURA M., ONO T. Submarine active normal faults completely crossing the southwest Ryukyu Arc. *Tectonophysics* in press, **2007**.
- 11 HAMAMOTO F., SAKURAI M., NAGANO M. Submarine geology off the Miyako and Yaeyama Islands, Report of Hydrographic Researches **14**, 1, **1979**.
- 12 THE RESEARCH GROUP FOR ACTIVE FAULTS OF JAPAN Maps of active faults in Japan with an explanatory text. University of Tokyo Press, Tokyo, pp. 74, **1992**.
- 13 NAKAMURA M. Source fault model of the 1771 Yaeyama Tsunami, Southern Ryukyu Islands, Japan, inferred from numerical simulation. *Pure and Applied Geophysics* **163**, 41, **2006**.
- 14 KUBO A., FUKUYAMA E. Stress field along the Ryukyu arc and the Okinawa trough inferred from moment tensors of shallow earthquakes. *Earth. Planet. Sci. Lett.* **210**, 305, **2003**.
- 15 MATSUMOTO T. An underwater landslide or slump on an active submarine fault - a possible source of a devastating tsunami? *Eos Trans. AGU* 88 (52), Fall Meet. Suppl., Abstract S53A-1018, **2007**.